Advances in Nano Research, *Vol. 6 No. 2 (2018) 163-182*
DOI: https://doi.org/10.12989/anr.2018.6.2.163

Nonlinear vibration analysis of an embedded multi-walled carbon nanotube

Chih-Ping Wu *, Yan-Hong Chen, Zong-Li Hong and Chia-Hao Lin

Department of Civil Engineering, National Cheng Kung University, Taiwan, ROC

(*Received January 25, 2017, Revised April 7, 2018, Accepted June 17, 2018*)

Abstract. Based on the Reissner mixed variational theorem (RMVT), the authors present a nonlocal Timoshenko beam theory (TBT) for the nonlinear free vibration analysis of multi-walled carbon nanotubes (MWCNT) embedded in an elastic medium. In this formulation, four different edge conditions of the embedded MWCNT are considered, two different models with regard to the van der Waals interaction between each pair of walls constituting the MWCNT are considered, and the interaction between the MWCNT and its surrounding medium is simulated using the Pasternak-type foundation. The motion equations of an individual wall and the associated boundary conditions are derived using Hamilton's principle, in which the von Kármán geometrical nonlinearity is considered. Eringen's nonlocal elasticity theory is used to account for the effects of the small length scale. Variations of the lowest frequency parameters with the maximum modal deflection of the embedded MWCNT are obtained using the differential quadrature method in conjunction with a direct iterative approach.

Keywords: foundations; multi-walled carbon nanotubes; nonlinear vibration; nonlocal Timoshenko beams; Reissner's mixed variational theorem; van der Waals interaction

1. Introduction

Since carbon nanotubes (CNTs) were first discovered (Iijima 1991), the development of nanoscience and nanotechnologies, as well as application of CNTs to various advanced industries, has made remarkable progress due to the novel material properties of these structures, such as extremely high stiffness- and strength-to-weight ratios, high conductivity and remarkable electronic properties. Their potential applications in assorted technological areas include aerospace, automobile, energy, medicine, and chemical industry (Khare and Bose 2005). For examples, due to their superior metallic and semiconducting properties, CNTs have enabled some of highly promising electronic applications in nano-electro-mechanical systems, such as CNT-based sensors and actuators (Li *et al*. 2008). Because the effects of CNTs on the enhancement of the tribological properties of CNT-metal composites are significant, the Ni-P-CNT composite coating and CNT/copper matrix composites have been developed in the electroless plating and powder metallurgy techniques, respectively (Chen *et al*. 2003). A graphene-CNTs hybrid nanostructure was synthesized in the lithium ion battery application to strengthen its electrostatic interaction and cyclic stability (Vinayan *et al*. 2012). To improve the bonding performance between the graphene

*Corresponding author, Ph.D., Professor, E-mail: cpwu@mail.ncku.edu.tw

http://www.techno-press.org/?journal=anr&subpage=5 ISSN: 2287-237X (Print), 2287-2388 (Online)

fibers and epoxy matrix in the conventional fiber-reinforced composite plates/shells, the CNTs were dispersed in epoxy to produce desired toughened adhesives (Hsiao *et al*. 2003). There are still numerous applications of CNTs, such as drug delivery, chemical anti-oxidation, optoelectronics, and microfluidics (Bianco *et al*. 2005, Datsyuk *et al*. 2008), and some review articles with regard to the synthesis and properties of CNTs and their present and future commercial applications can be found in the literature (Harris 2009, Thostenson *et al*. 2001, De Volder *et al*. 2013).

Because CNTs possess great potential for high-end industrial applications as above mentioned, a variety of mechanical analyses of embedded and non-embedded single- double-, and multi-walled (SW, DW, and MW) CNTs have attracted considerable attention in order to enhance their structural performance and extend their working life. One of the most important research areas in such works is examining the linear and nonlinear vibration characteristics of SW, DW, and MW CNTs (Gibson *et al*. 2007). It is well known that the natural frequencies of a beam are independent of the maximum amplitude of their corresponding mode shapes in the cases of linear vibration behavior, while they are dependent upon the maximum amplitude of their corresponding mode shapes in the cases of geometrical nonlinear behavior, which often occurs when the maximum amplitude of the mode shape approaches the total thickness of the beam. To obtain the accurate solutions of the natural frequencies of the MWCNTs, it needs to account for the geometrical nonlinear effect in the corresponding vibration analysis.

In the open literature, there are basically four categories of simulation methods used to carry out these analyses, namely atomistic modelling, hybrid atomistic-continuum mechanics, experimental methods and continuum mechanics, with the first two being especially time-consuming and the third being expensive and hard to conduct. Classical continuum mechanics-based theories are thus reformulated by accounting for the effects of the small length scale to develop the nonlocal version of these, in which Eringen's nonlocal elasticity theory (ENET) (Eringen 1983, 2002, Eringen and Edelen 1972) is the most popular and widely used among various nonlocal continuum mechanics theories. Some comprehensive literature surveys with regard to the analyses of structural behaviors of embedded and non-embedded SW, DW, and MW CNTs using various simulation methods have been undertaken (Eltaher *et al*. 2016, Behera and Chakraverty 2016).

Based on the principle of virtual displacement (PVD), some classical beam theories have been reformulated to obtain their corresponding nonlocal version theories using the ENET to take account of the effects of the small length scale, such as the nonlocal Euler-Bernoulli beam theory (EBBT) (Reddy 2007, Reddy and Pang 2008), nonlocal Timoshenko beam theory (TBT) (Reddy 2007, Reddy and Pang 2008), nonlocal Reddy beam theory (RBT) (Reddy 2007, Thai 2012, Ebrahimi and Barati 2016a), nonlocal sinusoidal shear deformation beam theory (SSDBT) (Thai and Vo 2012), nonlocal hyperbolic shear deformation beam theory (HSDBT) (Aissani *et al*. 2015) and nonlocal general beam theory (GBT) (Aydogdu 2009). Among numerous ENET-based nonlocal beam theories used for the bending, vibration and buckling analyses of SW, DW, and MW CNTs with and without being embedded in an elastic medium, the PVD-based nonlocal TBT is commonly used in the open literature, and has been shown to yield satisfactory results (Ansari and Sahmani 2012, Behera and Chakraverty 2015, Pradhan 2012, Wang *et al*. 2006a, b).

The above-mentioned nonlocal beam theories have also extended to the nonlinear static and dynamic analyses of embedded and non-embedded SW, DW and MW CNTs. Reddy (2010) reformulated the EBT, TBT, and RBT using the ENET and von Kármán geometrical nonlinearity (VKGN), in which the nonlinear equilibrium equations of various nonlocal beam theories were obtained on the basis of the PVD. Within the framework of PVD-based nonlocal TBT combined

with the VKGN, Yang *et al*. (2010) and Ke *et al*. (2009) investigated the nonlinear vibration behavior of non-embedded SW and embedded DW CNTs with combinations of simply-supported and clamped edges. Based on the nonlocal EBT and SSDBT, Fang *et al*. (2013) and Pour *et al*. (2015) presented the nonlinear vibration analysis of embedded DWCNTs with clamped-clamped edges, respectively, in which the interaction between the CNTs and the surrounding medium, as well as the vdW interactive forces between adjacent walls, were considered. Based on the nonlocal TBT, Ansari and Ramezannezhad (2011) studied the large-amplitude vibration behavior of an embedded MWCNT in thermal environments. The vdW interactive forces between adjacent and non-adjacent walls were taken into account.

Various coupled multi-fields analyses of both laminated composite and multilayered functionally graded (FG) structures have been carried out in the open literature, such as coupled magneto-electro-elastic, electro-elastic, thermo-elastic, thermo-piezo-elastic analyses (Huang *et al*. 2007, Pan and Han 2005, Sladek *et al*. 2015, Wu and Tsai 2007). Because SWCNTs and MWCNTs possess superior physical and chemical material properties as compared with the above mentioned composite materials, they have wildly been used in Nano- and Micro-Electro-Mechanical systems (NEMS and MEMS). The subjects with regard to assorted coupled multi-fields analyses of SWCNTs, MWCNTs, and FG nanobeams thus attract much attention due to the academic interests and practical application. Ebrahimi and Salari (2015a, 2016) presented Navier's solutions for the coupled thermo-mechanical vibration analysis of power-law-type FG nanobeams using a semi-analytical differential transform method (DTM), in which the nonlocal EBBT and TBT were used and the material properties were assumed to be temperature-dependent, which is more realistic in practice. In conjunction with the nonlocal RBT and DTM, Ebrahimi and Salari (2015b) investigated the coupled thermo-mechanical vibration of an SWCNT embedded in an elastic medium. On the basis of a refined trigonometric beam theory, Ebrahimi and Barati (2016b) investigated the magneto-electro-viscoelastic analysis of power-law-type FG nanobeams with different boundary conditions. Based on a nonlocal parabolic third-order shear deformation theory, Ebrahimi and Barati (2016c, 2018) undertook the coupled magneto-thermo-piezoelectro-mechanical free vibration analysis of power-law-type FG nanobeams, in which the effects of various temperature changes, applied magnetic potential and electric voltage, material-property gradient index, nonlocal parameters, and aspect ratios on the vibration behavior of the nanobeam are significant.

A competitive semi-numerical analytical method, the so-called differential transformation method (DTM), has also introduced to the nonlocal vibration analysis of FG nanobeams, even though application of the DTM to assorted structural analyses of macrobeams/plates/shells is available in the public literature (Hassan 2002, 2008a, b, Yalcin *et al*. 2009), while it is seldom extended to those of nanostructures. In the DTM, the strong form of a physical problem including the Euler-Lagrange equations (the system partial equations) and the associated natural and essential boundary conditions is transformed into a set of algebraic equations using the finite Taylor series, and it is illustrated to be an efficient technique to obtain the numerical and analytical solutions of both linear and nonlinear differential equations. By means of the DTM combined with the ENET, Ebrahimi *et al*. (2015), Ebrahimi and Shafiei (2016) and Ebrahimi and Salari (2015c) investigated the nonlocal vibration analysis of FG rotating and non-rotating nanobeams.

After a close survey of the open literature, the authors found that almost all of the nonlocal beam theories used for the analysis of SW, DW, and MW CNTs were derived on the basis of the PVD, rather than Reissner's mixed variational theorem (RMVT) (Reissner 1984, 1986), even though the RMVT-based theories were concluded to be superior to the PVD-based theories for use

with macro-scale structures by Carrera (2000, 2004). Wu and Lai (2015a, b) thus developed an RMVT-based nonlocal TBT for the linear bending and vibration analyses of SWCNTs embedded in an elastic medium and with various boundary conditions. Unlike the PVD-based models, in which the generalized displacement components (i.e., the in- and out-of-surface displacement and rotation) are regarded as the primary variables, the generalized resultant forces (i.e., axial force, shear force and bending moment) are also regarded as the primary variables in the RMVT-based models. The highest differential order of the Euler-Lagrange equations in the RMVT-based strong and weak formulations is thus one-half lower than that of those in the PVD-based ones. Impositions of the natural boundary conditions for the RMVT-based nonlocal TBT are more straight-forward than those for the PVD-based nonlocal one. Implementation of the RMVT- and PVD-based nonlocal TBTs showed that their solutions are in excellent agreement with the accurate solutions available in the open literature, while the convergence rate of the RMVT-based nonlocal TBT is faster than that of the PVD-based nonlocal one, and the RMVT-based nonlocal TBT is less time-consuming than the PVD-based one.

In this article, we extend the earlier work regarding the linear vibration analysis of embedded SWCNTs to the nonlinear vibration of embedded SW, DW, and MW CNTs when considering the VKGN and vdW interaction. The motion equations of an individual wall of the MWCNT and associated boundary conditions are derived using the Hamilton principle. Four different edge conditions of the embedded MWCNT, as well as two different models with regard to the vdW interactive forces between either adjacent walls only or any pair of walls constituting the MWCNT, are taken into account. The Pasternak-type foundation is used to simulate the interaction between the MWCNT and its surrounding medium. Moreover, a parametric study related to the influence of some factors on the lowest frequency parameters varying with the maximum modal deflection of the MWCNT and their corresponding spatial distributions of modal variables is undertaken, such as the effects of the small length scale, vdW interaction, aspect ratios, different boundary conditions, and the Winkler stiffness and shear modulus of the foundation.

2. The nonlinear RMVT-based local TBT

2.1 Kinematic and kinetic assumptions

In this work the nonlinear vibration characteristics of a moderately thick N_l –walled CNT resting on a two-parameter Pasternak foundation model are investigated, in which N_l denotes the total number of walls constituting the MWCNT, counted from the innermost wall to the outermost one. The thickness and mid-surface radius of the k^{th}-wall of the MWCNT are h_k and R_k ($k = 1 - N_l$), and the length of the MWCNT is L. A set of Cartesian coordinates (x, y, z) is located at the center of the MWCNT. The configuration, coordinates and kinematics of the k^{th}-wall CNT are given in Fig. 1. The interactive forces between a DWCNT and its surrounding medium and the vdW interactive forces mutually applied between adjacent walls constituting the DWCNT are shown in Fig. 2.

In the TBT, the shear deformation effect is considered to be a constant through the thickness coordinate of each individual wall, and the related displacement field of the k^{th}-wall of the MWCNT is given as follows

$$u_1^k(x, z, t) = u_k(x, t) - z\,\phi_k(x, t), \tag{1}$$

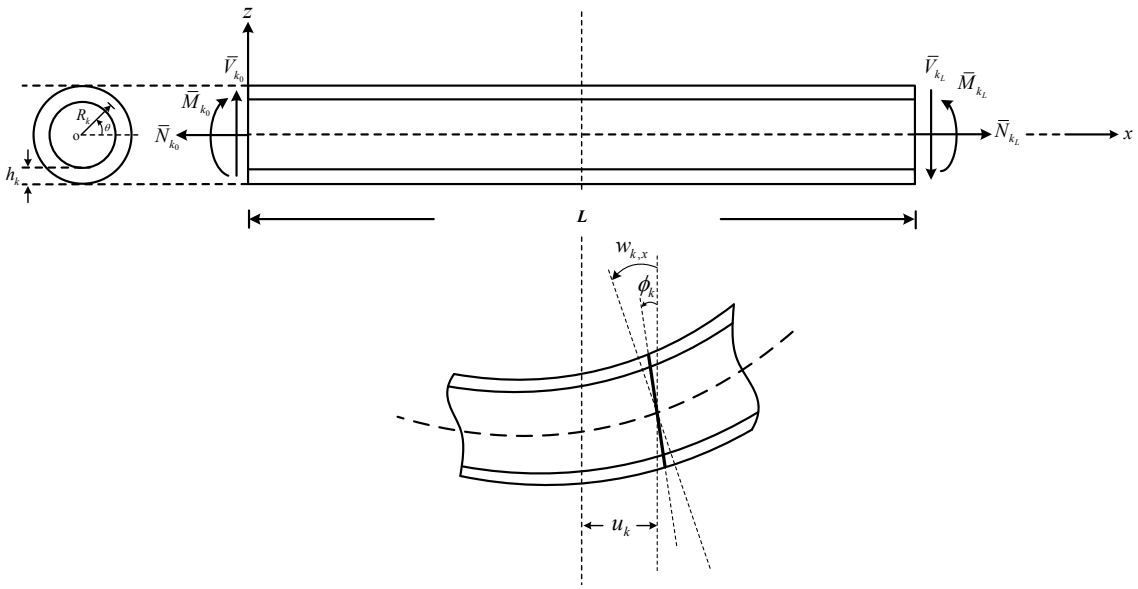

Fig. 1 The configuration, coordinates and kinematics of the k^{th}-wall of an MWCNT

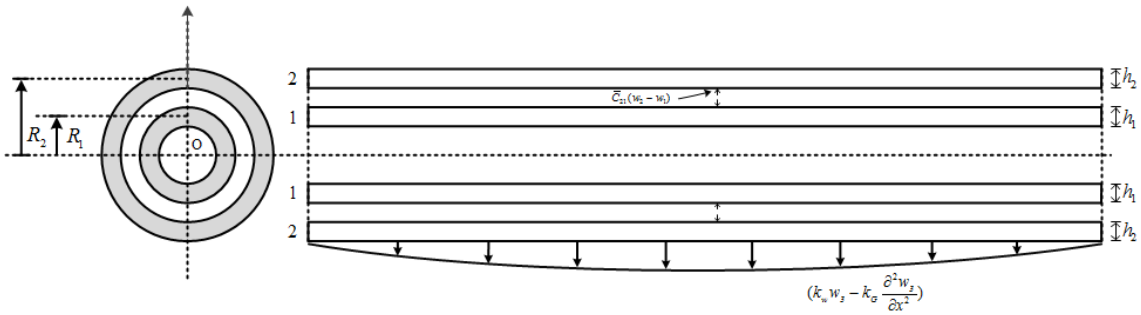

Fig. 2 The interactive forces between a DWCNT and its surrounding medium, and the vdW interactive forces mutually applied between adjacent walls constituting the DWCNT

$$u_2^k(x, z, t) = 0, \tag{2}$$

$$u_3^k(x, z, t) = w_k(x, t), \tag{3}$$

where u_i^k (i = 1 – 3) denote the displacement components of the k^{th}-wall in the x, y and z directions, respectively. u_k and w_k stand for the mid-surface displacement components of the k^{th}-wall in the x and z directions, and ϕ_k is the total rotation of the k^{th}-wall in the x-z plane. The deformation of a section in the y-z plane is shown in Fig. 1.

The strain-displacement relations of the k^{th}-wall CNT accounting for the VKGN are given by

$$\varepsilon_x^k = u_{k,x} - z\phi_{k,x} + (1/2)(w_{k,x})^2, \tag{4}$$

$$\gamma_{xz}^{k} = -\phi_k + w_{k,x}, \tag{5}$$

$$\varepsilon_y^k = \varepsilon_z^k = \gamma_{yz}^k = \gamma_{xy}^k = 0, \tag{6}$$

where ε_x^k, ε_y^k, ε_z^k, γ_{xz}^k, γ_{yz}^k and γ_{xy}^k are the strain components of the k^{th}-wall CNT, and the commas represent partial differentiation with respect to the suffix variables.

The nonzero stress components of the k^{th}-wall CNT in the local TBT are given by

$$\sigma_x^k = E_k \left\lfloor u_{k,x} - z\phi_{k,x} + (1/2)(w_{k,x})^2 \right\rfloor, \tag{7}$$

$$\tau_{xz}^k = k_{ck} G_k (-\phi_k + w_{k,x}), \tag{8}$$

in which E_k and G_k are the Young's and the shear moduli of the k^{th}-wall CNT, respectively. k_{ck} denotes the shear stress correction factor of the k^{th}-wall, which accounts for the non-uniform shear stress distribution through the thickness direction, and the value of k_{ck} will depend on the cross section and Poisson's ratio, and is reviewed by Cowper (1966), which is $k_{ck} = \dfrac{6(1+\upsilon_k)(1+c_{rk}^2)^2}{(7+6\upsilon_k)(1+c_{rk}^2)^2 + (20+12\upsilon_k)c_{rk}^2}$, in which $c_{rk} = (R_k - 0.5h_k)/(R_k + 0.5h_k)$.

The axial force (N_k), moment (M_k) and shear force (Q_k) resultants of the k^{th}-wall CNT are defined by

$$N_k = \int_{A_k} \sigma_x^k \, dA_k, \tag{9a}$$

$$M_k = -\int_{A_k} \sigma_x^k \, z \, dA_k, \tag{9b}$$

$$Q_k = -\int_{A_k} \tau_{xz}^k \, dA_k, \tag{9c}$$

Using Eqs. (9a)-(9c), we can express the stress components (σ_x^k and τ_{xz}^k) in terms of the axial force, bending moment and shear force of the k^{th}-wall CNT as follows

$$\sigma_x^k = \frac{N_k}{A_k} - z\frac{M_k}{I_k}, \tag{10a}$$

$$\tau_{xz}^k = -\frac{Q_k}{A_k}. \tag{10b}$$

where A_k and I_k denote the cross-sectional area and the area moment of inertia of the k^{th}-wall CNT.

2.2 Van der Waals interactive forces

Two different models with regard to the vdW interactive forces between either any pair of

walls constituting the MWCNT or adjacent walls only are considered in this work, and are given as follows:

2.2.1 The He et al. (2005a, b) Model

In He *et al*. (2005a, b), for an MWCNT the vdW interactive force (q_{ij}) of the i^{th}-wall exerted from the j^{th}-wall of the MWCNT is expressed as $q_{ij} = \overline{C}_{ij}\,\Delta w_{ij}$, in which Δw_{ij} is the relative displacement between the i^{th}- and j^{th}-walls and $\overline{C}_{ij}$ is the vdW interaction coefficient. According to He *et al*. (2005a, b), $\overline{C}_{ij}$ is given in the following form

$$\overline{C}_{ij} = -\left[\frac{1001\pi\varepsilon\sigma^{12}}{3a^4}E_{ij}^{13} - \frac{1120\pi\varepsilon\sigma^{6}}{9a^4}E_{ij}^{7}\right]R_j, \tag{11}$$

where R_j is the mid-surface radius of the j^{th}-wall of the MWCNT, a is the C-C bond length, and a = 0.142 mm, ε = 2.968 meV = 4.7488×10^{-22} J, σ = 0.3407 mm, and

$$E_{ij}^{m} = \left(R_i + R_j\right)^{-m}\int_0^{\pi/2}\left[1 - K_{ij}\cos^2\theta\right]^{-m/2}d\theta, \tag{12}$$

$$K_{ij} = 4R_iR_j\left(R_i + R_j\right)^{-2}. \tag{13}$$

Because the vdW interaction coefficient $\overline{C}_{ij}$ with a unit of nN/(nm)^3 is derived using a cylindrical shell model, it cannot be directly applied to the current nonlocal TBT. The equivalent vdW interaction coefficient C_{ij} with a unit nN/(nm)^2 for a beam model is thus derived as follows (Wu *et al*. 2017)

$$\begin{aligned} 4\int_0^{\pi/2}\overline{C}_{ij}\,\Delta w_{ij}\,R_i\sin^2\theta\,d\theta &= \left(\pi R_i\,\overline{C}_{ij}\right)\Delta w_{ij} \\ &= C_{ij}\,\Delta w_{ij}, \end{aligned} \tag{14}$$

where C_{ij} is obtained as $C_{ij} = \left(\pi R_i\right)\overline{C}_{ij}$.

2.2.2 The Ru model

The main difference between the He *et al*. and Ru models (He *et al*. 2005a, b, Ru 2000) is that in the former the vdW interactive forces are mutually applied between any pair of walls constituting the MWCNT, while in the latter these are mutually applied between adjacent walls only.

In order to have the same definition and sign for the vdW interactive forces used in the He *et al*. model, the authors change the sign for the vdW coefficient of the Ru model, multiply it with a correction factor (πR_{i+1}), and express it in the following form

$$C_{i(i+1)} = C_{(i+1)i} = -\left(\pi R_{i+1}\right)\left[\frac{320\left(2R_i\right)\text{erg}/\left(\text{cm}^2\times\text{nm}\right)}{\left(0.16\Delta^2\right)}\right], \tag{15}$$

where $i = 1 - (N_l - 1)$, Δ = 0.142 nm, and 1 erg = 10^{-7} (N·m). The units of R_i and R_{i+1} are nms, and $C_{kl} = 0$ when $l \neq (k-1)$ or $(k+1)$.

2.3 Hamilton's principle

Hamilton's principle is used to derive the motion equations of the geometrically nonlinear RMVT-based local TBT, and the corresponding energy functional (I_R) for the dynamic version of the geometrically nonlinear RMVT-based local TBT is written in the form of

$$I_R = \int_{t_1}^{t_2} (T - \Pi_R) dt, \tag{16}$$

where T and Π_R denote the kinetic energy and Reissner's strain energy functions, and t is the time variable. $T = \sum_{k=1}^{N_l} T_k$ and $\Pi_R = \sum_{k=1}^{N_l} (\Pi_R)_k$, in which T_k and $(\Pi_R)_k$ are the kinetic energy and Reissner's strain energy functions of the k^{th}-wall CNT, and these are given as follows

$$\begin{aligned} T_k &= \int_0^L \iint_{A_k} (\rho/2)\left[(u_1^k{}_{,t})^2 + (u_2^k{}_{,t})^2 + (u_3^k{}_{,t})^2\right] dA_k\, dx \\ &= \int_0^L \left\{(1/2)\left[m_{k0}(u_{k,t})^2 + m_{k2}(\phi_{k,t})^2 + m_{k0}(w_{k,t})^2\right]\right\} dx, \end{aligned} \tag{17}$$

$$\begin{aligned} (\Pi_R)_k &= \int_0^L \int_{A_k} [\sigma_x^k \varepsilon_x^k + \tau_{xz}^k \gamma_{xz}^k - (\sigma_x^k)^2/(2E_k) - (\tau_{xz}^k)^2/(2k_{ck}G_k)] dA_k\, dx \\ &\quad + \delta_{kN_l} \int_0^L (1/2)\left[k_w (w_k)^2 + k_G (w_{k,x})^2\right] dx \\ &\quad + \int_0^L q_{vdW}^k w_k\, dx + \overline{N}_{k0} u_{k0} - \overline{N}_{kL} u_{kL} + \overline{M}_{k0} \phi_{k0} - \overline{M}_{kL} \phi_{kL} - \overline{V}_{k0} w_{k0} + \overline{V}_{kL} w_{kL} \\ &= \int_0^L \left\{N_k u_{k,x} + (N_k/2)(w_{k,x})^2 - \left[(N_k)^2/(2A_k E_k)\right] + M_k \phi_{k,x}\right. \\ &\qquad \left. - \left[(M_k)^2/(2E_k I_k)\right] + Q_k(\phi_k - w_{k,x}) - \left[(Q_k)^2/(2k_{ck} G_k A_k)\right]\right\} dx \\ &\quad + \delta_{kN_l} \int_0^L (1/2)\left[k_w (w_k)^2 + k_G (w_{k,x})^2\right] dx \\ &\quad + \int_0^L q_{vdW}^k w_k\, dx + \overline{N}_{k0} u_{k0} - \overline{N}_{kL} u_{kL} + \overline{M}_{k0} \phi_{k0} - \overline{M}_{kL} \phi_{kL} - \overline{V}_{k0} w_{k0} + \overline{V}_{kL} w_{kL}, \end{aligned} \tag{18}$$

in which ρ is the mass density of the CNT, and the inertias m_{k0} and m_{k2} are defined as $m_{k0} = \iint_{A_k} \rho\, dA_k$ and $m_{k2} = \iint_{A_k} \rho\, z^2\, dA_k$. k_w and k_G are the Winkler stiffness and shear modulus of the surrounding elastic medium, respectively, and $\overline{N}_{k0}, \overline{N}_{kL}$, $\overline{M}_{k0}, \overline{M}_{kL}$, $\overline{V}_{k0}$ and $\overline{V}_{kL}$ denote the applied axial forces, moments and shear forces of the k^{th}-wall CNT at the edges, and are shown in Fig. 1. δ_{kl} is the Dirac delta function, in which $\delta_{kl} = 1$ when $k = l$, while $\delta_{kl} = 0$ when $k \neq l$. q_{vdW}^k denotes the total vdW interactive forces of the k^{th}-wall CNT exerted from other walls, respectively, the positive direction of which is defined to be downward. The term $q_{vdW}^k\, \delta w_k$ is given as follows

$$q_{vdW}^{k}\ \delta w_k = \left[\sum_{\substack{l=1 \\ (l\neq k)}}^{N_l} \left(C_{kl} w_l\right) - \left(\sum_{\substack{l=1 \\ (l\neq k)}}^{N_l} C_{kl} \right) w_k \right] \delta w_k, \tag{19}$$

where C_{kl} denotes the vdW interaction coefficient. For an MWCNT, C_{kl} of the He *et al*. and Ru models are given in Eqs. (11)-(14) and (15), respectively (He *et al*. 2005a, b, Ru 2000).

Performing the first-order variation of the above-mentioned energy functional (I_R), using integration by parts, and then imposing the stationary principle of the above-mentioned energy functional (i.e., $\delta I_r = 0$), the authors obtain the motion equations of the geometrically nonlinear RMVT-based local TBT and the possible boundary conditions as follows:

Motion equations in the interior domain of the k^{th}-wall CNT ($0 < x < L$)

$$\delta u_k :\ -N_{k,x} = -m_{k0}\, u_{k,tt}, \tag{20}$$

$$\delta w_k :\ Q_{k,x} - N_{k,x}\, w_{k,x} - N_k\, w_{k,xx} = -q_{vdW}^{k} - \delta_{kN_l}\left(k_w\, w_k - k_G\, w_{k,xx}\right) - m_{k0}\, w_{k,tt}, \tag{21}$$

$$\delta \phi_k :\ -M_{k,x} + Q_k = -m_{k2}\, \phi_{k,tt}, \tag{22}$$

$$\delta N_k :\ N_k - A_k E_k \left[u_{k,x} + (1/2)\left(w_{k,x}\right)^2\right] = 0, \tag{23}$$

$$\delta M_k :\quad M_k - E_k\, I_k\, \phi_{k,x} = 0, \tag{24}$$

$$\delta Q_k :\ Q_k - k_{ck}\, G_k A_k \left(\phi_k - w_{k,x}\right) = 0, \tag{25}$$

where $k = 1, 2, \ldots, N_l$.

Possible boundary conditions at the edges of the MWCNT

At $x = 0$, either

$$u_{k0} = \overline{u}_{k0} \quad \text{or} \quad N_{k0} = \overline{N}_{k0}, \tag{26a}$$

either

$$w_{k0} = \overline{w}_{k0} \quad \text{or} \quad Q_{k0} - N_{k0}\left(w_{k0,x}\right) - \delta_{kN_l} k_G \left(w_{k0,x}\right) = \overline{V}_{k0}, \tag{26b}$$

either

$$\phi_{k0} = \overline{\phi}_{k0} \quad \text{or} \quad M_{k0} = \overline{M}_{k0}; \tag{26c}$$

At $x = L$, either

$$u_{kL} = \overline{u}_{kL} \quad \text{or} \quad N_{kL} = \overline{N}_{kL}, \tag{27a}$$

either

$$w_{kL} = \overline{w}_{kL} \quad \text{or} \quad Q_{kL} - N_{kL}\left(w_{kL,x}\right) - \delta_{kN_l} k_G \left(w_{kL,x}\right) = \overline{V}_{kL}, \tag{27b}$$

either

$$\phi_{kL} = \overline{\phi}_{kL} \quad \text{or} \quad M_{kL} = \overline{M}_{kL}. \tag{27c}$$

3. The geometrically nonlinear RMVT-based nonlocal TBT

3.1 Eringen's nonlocal constitutive relations

In the nonlocal elasticity theory, the stress components induced at a particular material point of the loaded elastic body will depend on the strain components induced at all the material points of the continuum, due to the effects of the small length scale. According to ENET, the nonlocal constitutive behavior of an elastic body can be written as

$$\left(1 - \mu \nabla^2\right)\sigma_{ij} = c_{ijkl}\, \varepsilon_{kl}, \tag{28}$$

where μ denotes the nonlocal parameter, and $\mu = (e_0 a_0)^2$, in which a_0 is the internal characteristic length and e_0 is a constant used to adjust the nonlocal continuum model by matching its results with some of the reliable results obtained by experiments or other models. c_{ijkl} are the stiffness coefficients of the elastic beam-like solid, and σ_{ij} and ε_{kl} are the stress and strain components, respectively.

Using Eq. (28), the author can write the constitutive equations of the k^{th}-wall CNT for the nonlocal Timoshenko beam theory, as follows

$$\sigma_x^k - \mu \sigma_{x,xx}^k = E_k\, \varepsilon_x^k, \tag{29}$$

$$\tau_{xz}^k - \mu \tau_{xz,xx}^k = k_{ck}\, G_k\, \gamma_{xz}^k, \tag{30}$$

Using Eqs. (29) and (30) in conjunction with Eqs. (9a)-(9c), we can express the axial force, bending moment and shear force resultants of the k^{th}-wall CNT in terms of the generalized displacement components as

$$N_k - \mu N_{k,xx} = A_k E_k \left[u_{k,x} + (1/2)\left(w_{k,x}\right)^2\right], \tag{31}$$

$$M_k - \mu M_{k,xx} = E_k I_k\, \phi_{k,x}, \tag{32}$$

$$Q_k - \mu Q_{k,xx} = k_{ck}\, G_k\, A_k \left(\phi_k - w_{k,x}\right). \tag{33}$$

Eqs. (31)-(33) combined with Eqs. (20)-(22) constitute the set of motion equations of the geometrically nonlinear RMVT-based nonlocal TBT, and Eqs. (26a)-(26c) and (27a)-(27c) are the possible boundary conditions at the edges. These equations constitute the strong formulation of the dynamic version of the geometrically nonlinear nonlocal TBT, and are a well-posed eigen-value problem for the nonlinear free vibration analysis of an embedded MWCNT with different

boundary conditions.

4. Applications

In this section, the primary variables are expressed as a harmonic function in the time domain, and then the DQ method (Du *et al*. 1994, Wu and Lee 2001) is used to construct the weighting coefficients for the first- and higher-order derivatives of the primary variables in the spatial (x) domain, such that

$$\left.\frac{\partial F^r(x,t)}{\partial x^r}\right|_{x=x_i} = \left(\sum_{j=1}^{n_p} A_{ij}^{(r)} F_j\right) e^{i\omega t}, \tag{34}$$

where $r \geq 1$, $F_j = (u_k)_j$, $(w_k)_j$, $(\phi_k)_j$, $(N_k)_j$, $(M_k)_j$ and $(Q_k)_j$. ω denotes the natural frequency of the embedded MWCNT.

Applying the DQ formulae (i.e., Eq. (34)) to the strong formulation for the nonlinear free vibration problem of an embedded MWCNT based on the geometrically nonlinear RMVT-based nonlocal TBT, the authors obtain a set of simultaneous nonlinear algebraic equations, in which four different boundary conditions will be considered, such as the simple-simple (SS), clamped-clamped (CC) and clamped-simple (CS) and clamped-free (CF) supports.

Applying the DQ formulae to the motion equations at the sampling nodes in the interior domain, and satifying the associated boundary conditions at two edges, we finally obtain a set of $6(n_p - 1)N_l$ simultaneously algebraic equations in terms of $6(n_p - 1)N_l$ unknowns, which represents a standard nonlinear eigenvalue problem. Because a direct iterative method is used to solve these nonlinear equations, they are rewritten in the matrix form as follows

$$\left(\begin{bmatrix} \mathbf{K}_{11}^{(m)} & \mathbf{K}_{12}^{(m)} \\ \mathbf{K}_{21}^{(m)} & \mathbf{K}_{22}^{(m)} \end{bmatrix} + \begin{bmatrix} \mathbf{G}_{11}^{(m-1)} & \mathbf{0} \\ \mathbf{G}_{21}^{(m-1)} & \mathbf{0} \end{bmatrix} - \omega^2 \begin{bmatrix} \mathbf{M}_{11}^{(m)} & \mathbf{0} \\ \mathbf{0} & \mathbf{0} \end{bmatrix}\right) \begin{Bmatrix} \mathbf{X}_1^{(m)} \\ \mathbf{X}_2^{(m)} \end{Bmatrix} = \begin{Bmatrix} \mathbf{0} \\ \mathbf{0} \end{Bmatrix}, \tag{35}$$

where the superscript m denotes the m^{th} iteration. The coefficients $\mathbf{G}_{11}^{(m-1)}$ and $\mathbf{G}_{21}^{(m-1)}$ are in terms of the determined variables $\mathbf{X}_1^{(m-1)}$ and $\mathbf{X}_2^{(m-1)}$, and let $\mathbf{G}_{11}^{(0)} = \mathbf{G}_{21}^{(0)} = \mathbf{0}$, which means the linear solutions will be used as the initial guess of the unknowns to obtain the nonlinear ones, i.e., the convergent solutions obtained from the direct iterative method with an allowable error $\in_\alpha$ less than 10^{-5}, in which the allowable error $\in_\alpha$ is defined as $\in_\alpha = \sqrt{\left(\mathbf{X}^{(m)} - \mathbf{X}^{(m-1)}\right) \bullet \left(\mathbf{X}^{(m)} - \mathbf{X}^{(m-1)}\right)} / \sqrt{\left(\mathbf{X}^{(m)}\right) \bullet \left(\mathbf{X}^{(m)}\right)}$, in which the symbol , $\bullet$, denotes the inner product operation for two vectors, and $\mathbf{X}^{(m)} = \left\{\mathbf{X}_1^{(m)} \ \mathbf{X}_2^{(m)}\right\}^T$.

A matrix partition process and a direct iterative method are performed to solve the natural frequencies of an embedded MWCNT with various boundary conditions. From the second equation in Eq. (35), one can obtain

$$\mathbf{X}_2^{(m)} = -\left(\mathbf{K}_{22}^{(m)}\right)^{-1} \left(\mathbf{K}_{21}^{(m)} + \mathbf{G}_{21}^{(m-1)}\right) \mathbf{X}_1^{(m)}. \tag{36}$$

Using Eq. (36), the authors can condense Eq. (35) in the following form of

$$\left[\left(\mathbf{K}_{11}^{(m)}+\mathbf{G}_{11}^{(m-1)}\right)-\mathbf{K}_{12}^{(m)}\left(\mathbf{K}_{22}^{(m)}\right)^{-1}\left(\mathbf{K}_{21}^{(m)}+\mathbf{G}_{21}^{(m-1)}\right)-\omega^2\,\mathbf{M}_{11}^{(m)}\right]\mathbf{X}_1^{(m)}=\mathbf{0}. \tag{37}$$

Eq. (37) represents a standard eigenvalue problem, and a nontrivial solution of this exists if the determination of the coefficient matrix vanishes. The natural frequencies can thus be obtained by

$$\left|\left(\mathbf{K}_{11}^{(m)}+\mathbf{G}_{11}^{(m-1)}\right)-\mathbf{K}_{12}^{(m)}\left(\mathbf{K}_{22}^{(m)}\right)^{-1}\left(\mathbf{K}_{21}^{(m)}+\mathbf{G}_{21}^{(m-1)}\right)-\omega^2\,\mathbf{M}_{11}^{(m)}\right|=\mathbf{0}. \tag{38}$$

Once Eq. (38) is solved, the corresponding eigenvectors, which consist of nodal generalized displacement and force resultant components for each wall, can thus be obtained. In this work, the authors approximately scaled up this eigenvector such that the maximum transverse displacement of the innermost wall is equal to a given vibration amplitude $(W_1)_{\max}$, which means the authors let $w_1(x = 0.5L) = (W_1)_{\max}$ in the SS and CC cases, while $w_1(x = 0.57L) = (W_1)_{\max}$ in the CS cases and $w_1(x = L) = (W_1)_{\max}$ in the CF cases. Using the scaled up eigenvector to determine the nonlinear coefficient matrices, i.e., $\mathbf{G}_{11}^{(m-1)}$ and $\mathbf{G}_{21}^{(m-1)}$, a new eigenvalue and eigenvector can be thus obtained by using the updated eigenvalue system equations (i.e., Eq. (35)). Using this iterative process, the authors can obtain the convergent solutions of the natural frequencies of the embedded MWCNT until the relative error between the natural frequencies (ω) of m^{th} and $(m\text{-}1)^{\text{th}}$ iterations and that between the mean-square norm of the scaled up displacement vector ($\mathbf{X}_1$)of m^{th} and $(m - 1)^{\text{th}}$ iterations are less than an allowable error, which is 10^{-5} in this work.

5. Illustrative examples

5.1 Non-embedded DWCNTs

The linear vibration characteristics of a non-embedded DWCNT with combinations of simply supported and clamped boundary conditions have been examined by Ke *et al*. (2009) using the PVD-based nonlocal TBT, in which the vdW interaction of Ru's model was used. This issue was also studied by Ehteshami and Hajabasi (2011) and Shakouri *et al*. (2009) using the PVD-based nonlocal EBBT, as well as by Wang *et al*. (2006a) using the PVD-based nonlocal EBBT and TBT. These solutions of the frequency parameters of the DWCNT with assorted boundary conditions are used for assessing the accuracy of the current RMVT-based nonlocal TBT.

Table 1 shows the current DQ solutions of RMVT-based nonlocal TBT for the first three lowest frequency parameters ($\overline{\omega}$) of a DWCNT with different boundary conditions, in which μ = 0 and 1.96 nm^2, $\overline{\omega}=\sqrt[4]{\rho A_t L^4 \omega/(E I_t)}$, $A_t = A_1 + A_2$, $I_t = I_1 + I_2$, n_p = 15, and the values of k_{ck} (k = 1 and 2 are given using the formula from Cowper (1966).

The geometric parameters and material properties are the same as those used in Ke *et al*. (2009), which are $h_1 = h_2$ = 0.35 nm, L = 14 nm, $R_1 = R_2$ = 0.35 nm : 0.7 nm, E = 1000 GPa, υ = 0.25, ρ = 2.3×10^3 kg/m^3.

It can be seen in Table 1 that the solutions of the first three lowest frequency parameters of the non-embedded DWCNT obtained using the current RMVT-based nonlocal TBT agree closely with the solutions of Ke *et al*. (2009) and Wang *et al*. (2006a) obtained using the PVD-based nonlocal TBT. These solutions for the first mode are lower than the solutions obtained using the PVD-based nonlocal EBBT by about 0.64%, 1.3%, 3.1% and 5.2% for the cases of CF, SS, CS and CC edges,

Table 1 The DQ solutions of RMVT- based nonlocal TBT for the first three lowest frequency parameters ($\overline{\omega}$) of a DWCNT with various boundary conditions, and without foundation models

BCs	Theories	$\mu = 0$ (nm)^2			$\mu = 1.96$ (nm)^2		
		1st mode	2nd mode	3rd mode	1st mode	2nd mode	3rd mode
SS	[a]Wang *et al*. (2006a)	3.1410	6.2650	9.2756	NA	NA	NA
	Ehteshami and Hajabasi (2011)	3.141	6.265	9.276	3.068	5.770	7.976
	Shakouri *et al*. (2009)	3.1413	6.2735	9.3476	3.0683	5.7753	8.0060
	[b]Wang *et al*. (2006a)	3.0662	6.0378	8.5758	NA	NA	NA
	Ke *et al*. (2009)	3.099	NA	NA	3.027	NA	NA
	[c]Current linear	3.099	5.977	8.531	3.027	5.501	7.288
	[d]Current linear	3.099	5.974	8.513	3.027	5.499	7.281
CS	[a]Wang *et al*. (2006a)	3.9253	7.0355	9.9811	NA	NA	NA
	Ehteshami and Hajabasi (2011)	3.925	7.035	9.981	3.819	6.444	8.557
	Shakouri *et al*. (2009)	3.93	7.05	10.09	3.82	6.45	8.60
	[b]Wang *et al*. (2006a)	3.8598	6.7185	9.2148	NA	NA	NA
	Ke *et al*. (2009)	3.802	NA	NA	3.701	NA	NA
	[c]Current linear	3.802	6.539	8.954	3.702	5.997	7.631
	[d]Current linear	3.802	6.534	8.934	3.702	5.994	7.622
CC	Ehteshami and Hajabasi (2011)	4.726	7.796	10.654	4.590	7.105	9.123
	Shakouri *et al*. (2009)	4.73	7.82	10.82	4.59	7.12	9.19
	Ke *et al*. (2009)	4.482	NA	NA	4.359	NA	NA
	[c]Current linear	4.484	7.054	9.344	4.361	6.446	7.944
	[d]Current linear	4.483	7.047	9.322	4.360	6.441	7.935
CF	Ehteshami and Hajabasi (2011)	1.875	4.690	7.797	1.879	4.544	7.111
	Shakouri *et al*. (2009)	1.88	4.69	7.82	1.88	4.55	7.13
	[c]Current linear	1.863	4.502	7.021	1.867	4.359	6.537
	[d]Current linear	1.863	4.501	7.021	1.867	4.358	6.532

[a] The solutions are obtained by Wang *et al*. (2006a) using the PVD-based nonlocal EBBT
[b] The solutions are obtained by Wang *et al*. (2006a) using the PVD-based nonlocal TBT
[c] The solutions are obtained using the current RMVT-based nonlocal TBT and the vdW interaction model of Ru (2000)
[d] The solutions are obtained using the current RMVT-based nonlocal TBT and vdW interaction model of He *et al*. (2005a, b)

respectively, and these deviations between the frequency parameters obtained using the nonlocal EBBT and TBT become greater, i.e. the effect of shear deformation increases, for the higher modes. The effect of shear deformation will soften the gross stiffness of the DWCNT, and the effect of this on the frequency parameters of the DWCNT with different boundary conditions follow the order of CC > CS > SS > CF. Moreover, the results also show the solutions of the lowest frequency parameters of the DWCNT obtained using the vdW interaction models of Ru and He *et al*. are almost identical to each other.

For the future study purposes, the vdW coefficients of a five-walled CNT obtained using the

Table 2 vdW interaction coefficients C_{kl} (nN/nm^2) between the k^{th} and l^{th} walls of a five-walled CNT using the modified formulae of He *et al*. and Ru

	No. layers (N_l)	$l = 1$	$l = 2$	$l = 3$	$l = 4$	$l = 5$
$k = 1$	He *et al*. (2005a, b)	0	-92.3317	3.1698	0.3386	0.0690
	Ru (2000)	0	-152.6860	0	0	0
$k = 2$	He *et al*. (2005a, b)	-92.3317	0	-161.4667	5.0062	0.5107
	Ru (2000)	-152.6860	0	-458.0580	0	0
$k = 3$	He *et al*. (2005a, b)	3.1698	-161.4667	0	-228.7969	6.7941
	Ru (2000)	0	-458.0580	0	-916.1161	0
$k = 4$	He *et al*. (2005a, b)	0.3386	5.0062	-228.7969	0	-295.5899
	Ru (2000)	0	0	-916.1161	0	-1526.8601
$k = 5$	He *et al*. (2005a, b)	0.0690	0.5107	6.7941	-295.5899	0
	Ru (2000)	0	0	0	-1526.8601	0

modified formulae of He *et al*. (2005a, b) and Ru (2000) are listed in Table 2, in which the thickness of each wall are $h_1 = h_2 = h_3 = h_4 = h_5 = 0.35$ nm and the mid-surface radii of each wall are $R_1 : R_2 : R_3 : R_4 : R_5 = 0.35$ nm (1 : 2 : 3 : 4 : 5).

5.2 Embedded TWCNTs

In this section, the authors investigate the nonlinear vibration characteristics of embedded and non-embedded TWCNTs with SS and CC boundary conditions, in which the vdW interaction model of He *et al*. (2005a, b), Cowper's shear stress correction factor formula, and a Pasternak-type foundation model are used. The material properties of the CNT are $E = 1000$ GPa, $\upsilon = 0.25$, $\rho = 2300$ kg/m^3, and the effective thickness of each individual wall is $h_k = 0.35$ nm. A frequency parameter ratio between the nonlinear solutions and linear solutions for the i^{th} vibration mode is defined as $R_{\omega_i} = (\omega_i)_{nl} / (\omega_i)_l$. As mentioned before, the nonlinear solutions of the lowest frequency parameters are dependent upon the amplitude of the vibration mode, such that in the analysis the nonlinear solutions of frequency parameters will be obtained in association with a given value of the maximum modal deflection at $x = 0.5L$ of the innermost wall, i.e., $(W_1)_{max}$, for the SS and CC edges.

Fig. 3 shows variations of the frequency parameter ratios of the first mode ($(\omega_1)_{nl}/(\omega_1)_l$) of the non-embedded SW, DW and TW CNTs with the maximum modal deflection ($(W_1)_{max}$) for the cases of SS and CC edges, in which $\mu = 1$ (nm)^2, $L = 20$ nm, as well as $R_1 = 0.35$ nm $R_1 : R_2 = 0.35$ nm : 0.7 nm and $R_1 : R_2 : R_3 = 0.35$ nm : 0.7 nm : 1.05 nm for the SW, DW and TW CNTs, respectively. It is shown that the frequency parameter ratio increases when the value of the maximum modal deflection becomes greater. The geometrically nonlinear effect on the frequency parameters of non-embedded MWCNTs with different boundary conditions is SS > CC and SWCNT > DWCNT > TWCNT, in which the symbol ">" means more significant.

Fig. 4 shows variations of the frequency parameter ratios of the first mode of the non-embedded TWCNTs with the length-to-radius ratio (L/R_3) for the cases of SS and CC edges, in which $(W_1)_{max} = 0.6$ nm, $\mu = 0$, 1 and 2 (nm)^2 and $L/R_3 = 7 - 50$. It can be seen in Fig. 4 that the geometrically nonlinear effect will stiffen the TWCNT, such that the frequency parameter ratios

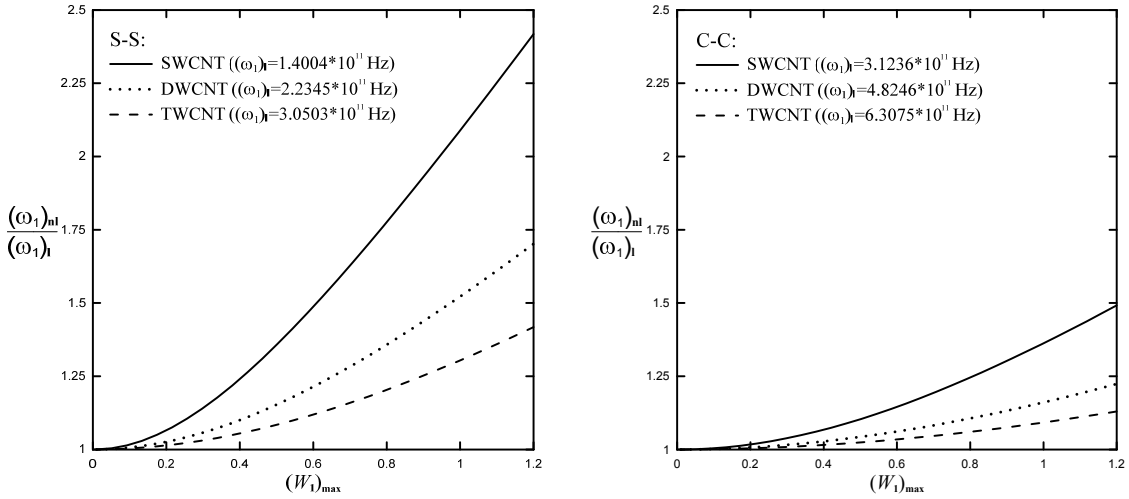

Fig. 3 Variations of the frequency parameter ratios of the first mode of non-embedded SW, DW and TW CNTs with maximum modal deflection: (a) SS; (b) CC supports

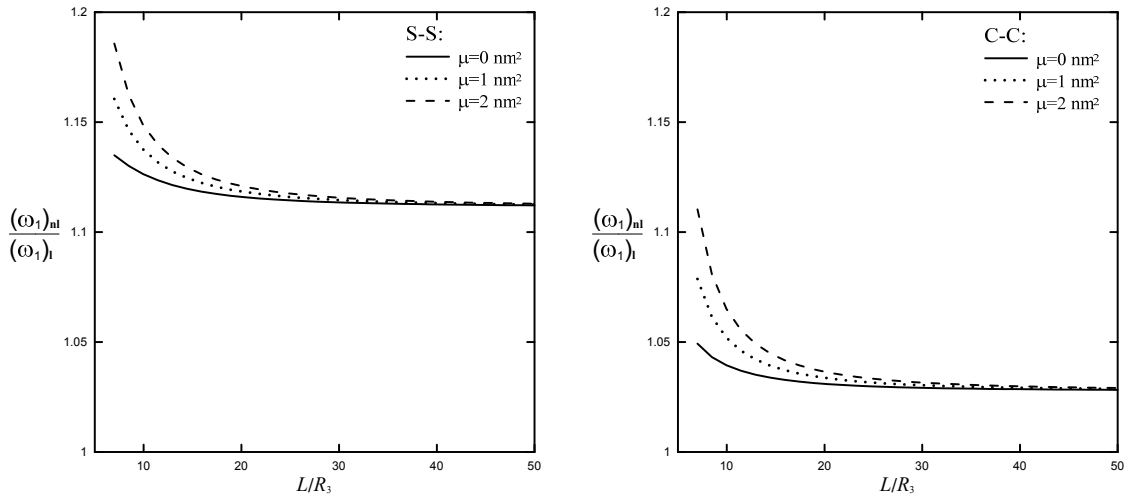

Fig. 4 Variations of the frequency parameter ratios of the first mode of non-embedded TWCNTs with the length-to-radius ratio: (a) SS; (b) CC supports

are always larger than 1, and this effect on the frequency parameters of the non-embedded TWCNT with short length is more significant than that seen on the one with long length.

Figs. 5 and 6 show variations of the frequency parameter ratios of the first mode of the embedded TWCNTs with the dimensionless Winkle spring stiffness (K_w) and the dimensionless shear modulus of the surrounding medium (K_G) for the cases of SS and CC edges, in which L = 20 nm, $(W_1)_{max}$ = 0.6 nm, μ = 0, 1 and 2 (nm)^2, as well as K_G = 0 and K_w = 100 in Figs. 5 and 6, respectively. It can be seen in Figs. 5 and 6 that the frequency parameter ratio decreases when the

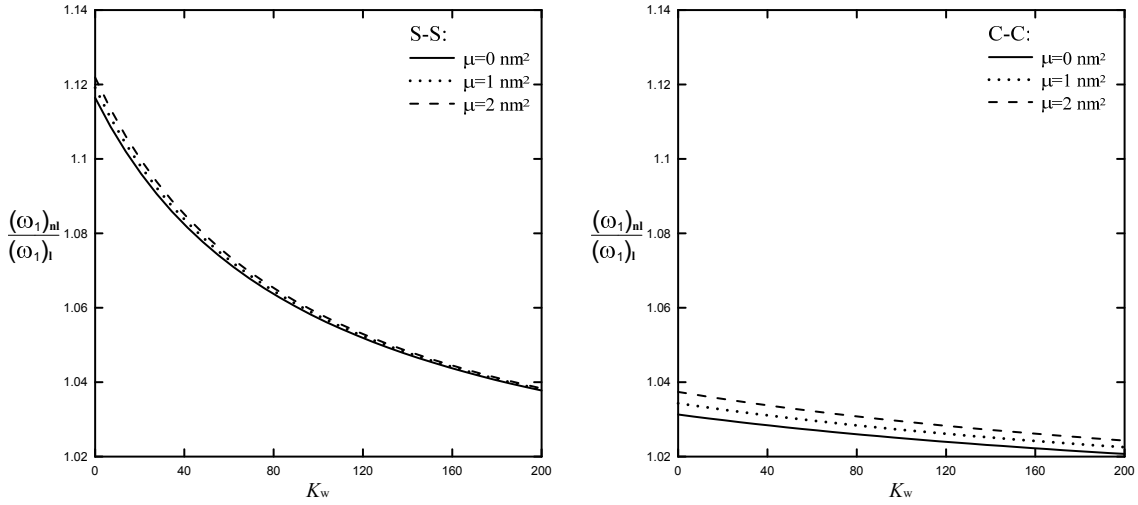

Fig. 5 Variations of the frequency parameter ratios of the first mode of embedded TWCNTs with the dimensionless Winkler stiffness: (a) SS; (b) CC supports

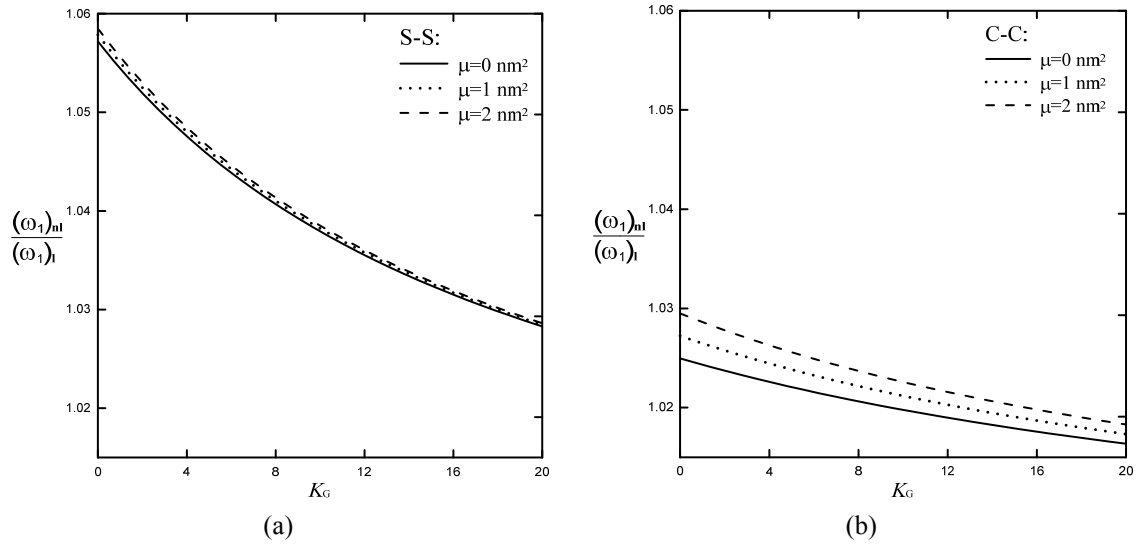

Fig. 6 Variations of the frequency parameter ratios of the first mode of embedded TWCNTs with the dimensionless shear modulus of the surrounding medium: (a) SS; (b) CC supports

values of K_w and K_G become greater. In contrast, the frequency parameter ratio increases when the nonlocal parameter becomes greater.

6. Conclusions

In this article the authors developed the RMVT-based nonlocal TBT for the nonlinear free

vibration analysis of embedded and non-embedded MWCNTs with various boundary conditions. The strong formulation of the RMVT-based nonlocal TBT and its associated possible boundary conditions for a typical individual wall are derived using the Hamilton principle, in which the generalized displacement (i.e., in- and out-of-surface displacement and total rotation) and generalized force (axial force, shear force and bending moment) variables of each wall are regarded as the primary variables, which differs from the PVD-based nonlocal TBT, in which the generalized displacement components of each individual wall are considered as the primary variables only. Two different formulae of vdW interactive forces, which are the He *et al*. and Ru models, derived from a nonlocal cylindrical shell model are modified to be suitable for the nonlocal beam model, and it is happy to see that the frequency parameters of MWCNTs obtained using the current RMVT-based nonlocal TBT combined with these two different models yield the identical results each other. The vdW interaction coefficients of a five-walled CNT obtained using the He *et al*. and Ru models are tabulated for future reference. In the numerical examples, it is shown that the solutions of the current RMVT-based nonlocal TBT converge rapidly and their convergent solutions are in excellent agreement with the accurate ones available in the literature. The results also show that the shear deformation effects on the frequency parameters of the MWCNTs for higher modes are more significant than those on the frequency parameters of MWCNTs for the first mode. The shear deformation effects will soften the gross stiffness of the MWCNTs, such that the frequency parameters of the MWCNTs obtained using the nonlocal TBT are always lower than those obtained using the nonlocal EBBT. The geometrical nonlinear effects on the frequency parameters of the MWCNTs become significant when the maximum amplitude of the modal shape of the MWCNTs approach the total thickness of the MWCNTs. Moreover, the different boundary conditions, nonlocal parameter, aspect ratio, and the Winkler stiffness and shear modulus of the surrounding medium significantly affect the free vibration behaviors of the embedded MWCNT.

Acknowledgments

This work was supported by the Ministry of Science and Technology of Republic of China through Grant MOST 103-2221-E-006-064-MY3.

References

Aissani, K., Bouiadjra, M.B., Ahouel, M. and Tounsi, A. (2015), "A new nonlocal hyperbolic shear deformation theory for nanobeams embedded in an elastic medium", *Struct. Eng. Mech., Int. J.*, **55**(4), 743-763.

Ansari, R. and Ramezannezhad, H. (2011), "Nonlocal Timoshenko beam model for the large-amplitude vibrations of embedded multiwalled carbon nanotubes including thermal effects", *Physica E*, **43**(6), 1171-1178.

Ansari, R. and Sahmani, S. (2012), "Small scale effect on vibrational response of single-walled carbon nanotubes with different boundary conditions based on nonlocal beam models", *Commun. Nonlin. Sci. Numer. Simul.*, **17**(4), 1965-1979.

Aydogdu, M. (2009), "A general nonlocal beam theory: Its application to nanobeam bending, buckling and vibration", *Physica E*, **41**(9), 1651-1655.

Behera, L. and Chakraverty, S. (2015), "Application of differential quadrature method in free vibration analysis of nanobeams based on various nonlocal theories", *Comput. Math. Appl.*, **69**(12), 1444-1462.

Behera, L. and Chakraverty, S. (2016), "Recent researches on nonlocal elasticity theory in the vibration of carbon nanotubes using beam models: A review", *Arch. Comput. Methods Eng.* DOI: 10.1007/s11831-016-9179-y

Bianco, A., Kostarelos, K. and Prato, M. (2005), "Applications of carbon nanotubes in drug delivery", *Current Opinion Chem. Biology*, **9**, 674-679.

Carrera, E. (2000), "An assessment of mixed and classical theories on global and local responses of multilayered orthotropic plates", *Compos. Struct.*, **50**(2), 183-198.

Carrera, E. (2004), "Assessment of theories for free vibration analysis of homogeneous and multilayered plates", *Shock Vib.*, **11**(3-4), 261-270.

Chen, W.X., Tu, J.P., Wang, L.Y., Gan, H.Y., Xu, Z.D. and Zhang X.B. (2003), "Tribological application of carbon nanotubes in a metal-based composite coating and composites", *Carbon*, **41**, 215-222.

Cowper, G. (1966), "The shear coefficient in Timoshenko's beam theory", *J. Appl. Mech.*, **33**(2), 335-340.

Datsyuk, V., Kalyva, M., Papagelis, K., Parthenios, J., Tasis, D., Siokou, A., Kallitsis, I. and Galiotis, C. (2008), "Chemical oxidation of multiwalled carbon nanotubes", *Carbon*, **46**, 833-840.

De Volder, M.F.L., Tawfick, S.H., Baughman, R.H. and Hart, A.J. (2013), "Carbon nanotubes: present and future commercial applications", *Sci.*, **339**, 535-539.

Du, H., Lim, M. and Lin, R. (1994), "Application of generalized differential quadrature method to structural problems", *Int. J. Numer. Methods Eng.*, **37**(11), 1881-1896.

Ebrahimi, F. and Barati, M.R. (2016a), "Analytical solution for nonlocal buckling characteristics of higher-order inhomogeneous nanosize beams embedded in elastic medium", *Adv. Nano Res., Int. J.*, **4**(3), 229-249.

Ebrahimi, F. and Barati, M.R. (2016b), "A nonlocal higher-order refined magneto-electro-viscoelastic beam model for dynamic analysis of smart nanostructures", *Int. J. Eng. Sci.*, **107**, 183-196.

Ebrahimi, F. and Barati, M.R. (2016c), "Dynamic modeling of a thermo-piezo-electrically actuated nanosize beam subjected to a magnetic field", *Appl. Phys. A*, **122**, 451 (18 pages).

Ebrahimi, F. and Barati, M.R. (2018), "Vibration analysis of smart piezoelectrically actuated nanobeams subjected to magneto-electrical field in thermal environment", *J. Vib. Control*, **24**(3), 549-564.

Ebrahimi, F. and Salari, E. (2015a), "Nonlocal thermo-mechanical vibration analysis of functionally graded nanobeams in thermal environment", *Acta Astronautica*, **113**, 29-50.

Ebrahimi, F. and Salari, E. (2015b), "Thermo-mechanical vibration analysis of a single-walled carbon nanotube embedded in an elastic medium based on higher-order shear deformation beam theory", *J. Mech. Sci. Technol.*, **29**(9), 3797-3803.

Ebrahimi, F. and Salari, E. (2015c), "Size-dependent free flexural vibrational behavior of functionally graded nanobeams using semi-analytical differential transform method", *Compos. Part B: Eng.*, **79**, 156-169.

Ebrahimi, F. and Salari, E. (2016), "Effect of various thermal loadings on buckling and vibrational characteristics of nonlocal temperature-dependent functionally graded nanobeams", *Mech. Adv. Mater. Struct.*, **23**(12), 1379-1397.

Ebrahimi, F. and Shafiei, N. (2016), "Application of Eringen's nonlocal elasticity theory for vibration analysis of rotating functionally graded nanobeams", *Smart Struct. Syst., Int. J.*, **17**(5), 837-857.

Ebrahimi, F., Ghadiri, M., Salari, E., Hoseini, S.A.H. and Shaghaghi, G.R. (2015), "Application of the differential transformation method for nonlocal vibration analysis of functionally graded nanobeams", *J. Mech. Sci. Technol.*, **29**(3), 1207-1215.

Ehteshami, H. and Hajabasi, M.A. (2011), "Analytical approaches for vibration analysis of multi-walled carbon nanotubes modeled as multiple nonlocal Euler beams", *Physica E*, **44**(1), 270-285.

Eltaher, M.A., Khater, M.E. and Emam, S.A. (2016), "A review on nonlocal elastic models for bending, buckling, vibrations, and wave propagation of nanoscale beams", *Appl. Math. Modell.*, **40**(5-6), 4109-4128.

Eringen, A.C. (1983), "On differential equations of nonlocal elasticity and solutions of screw dislocation and surface waves", *J. Appl. Phys.*, **54**(9), 4703-4710.

Eringen, A.C. (2002), *Nonlocal Continuum Field Theories*, Springer-Verlag, New York, USA.

Eringen, A.C. and Edelen, D.G.B. (1972), "On nonlocal elasticity", *Int. J. Eng. Sci.*, **10**, 233-248.
Fang, B., Zhen, Y.X., Zhang, C.P. and Tang, Y. (2013), "Nonlinear vibration analysis of double-walled carbon nanotubes based on nonlocal elasticity theory", *Appl. Math. Modell.*, **37**(3), 1096-1107.
Gibson, R.F., Ayorinde, E.O. and Wen, Y.F. (2007), "Vibrations of carbon nanotubes and their composites: A review", *Compos. Sci. Technol.*, **67**, 1-28.
Harris, P.J.F. (2009), *Carbon Nanotube Science*: *Synthesis*, *Properties and Applications*, Cambridge University Press, UK.
Hassan, I.H.A.H. (2002), "On solving some eigenvalue problems by using a differential transformation", *Appl. Math. Comput.*, **127**, 1-22.
Hassan, I.H.A.H. (2008a), "Application to differential transformation method for solving systems of differential equations", *Appl. Math. Modell.*, **32**, 2552-2559.
Hassan, I.H.A.H. (2008b), "Comparison differential transformation technique with Adomian decomposition method for linear and nonlinear initial value problems", *Chaos*, *Solitons Fractals*, **36**, 53-65.
He, X.Q., Kitipornchai, S. and Liew, K.M. (2005a), "Buckling analysis of multi-walled carbon nanotubes: a continuum model accounting for van der Waals interaction", *J. Mech. Phys. Solids*, **53**(2), 303-326.
He, X.Q., Kitipornchai, S., Wang, C.M. and Liew, K.M. (2005b), "Modeling of van der Waals force for infinitesimal deformation of multi-walled carbon nanotubes treated as cylindrical shells", *Int. J. Solids Struct.*, **42**(23), 6032-6047.
Hsiao, K.T., Alms, J. and Advani, S.G. (2003), "Use of epoxy/multiwalled carbon nanotubes as adhesives to join graphite fibre reinforced polymer composites", *Nanotechnol.*, **14**, 791-793.
Huang, D.J., Ding, H.J. and Chen, W.Q. (2007), "Analytical solution for functionally graded magneto-electro-elastic plane beams", *Int. J. Eng. Sci.*, **45**(2), 467-485.
Iijima, S. (1991), "Helica microtubes of graphitic carbon", *Nature*, **354**, 56-58.
Ke, L.L., Xiang, Y., Yang, J. and Kitipornchai, S. (2009), "Nonlinear free vibration of embedded double-walled carbon nanotubes based on nonlocal Timoshenko beam theory", *Comput. Mater. Sci.*, **47**(2), 409-417.
Khare, R. and Bose, S. (2005), "Carbon nanotube based composites-A review", *J. Miner. Mater. Character. Eng.*, **4**(1), 31-46.
Li, C., Thostenson, E.T. and Chou, T.W. (2008), "Sensors and actuators based on carbon nanotubes and their composites: A review", *Compos. Sci. Technol.*, **68**, 1227-1249.
Pan, E. and Han, F. (2005), "Exact solution for functionally graded and layered magneto-electro-elastic plates", *Int. J. Eng. Sci.*, **43**(3), 321-339.
Pour, H.R., Vossough, H., Beygipoor, M.M.H.G. and Azimzadeh, A. (2015), "Nonlinear vibration analysis of a nonlocal sinusoidal shear deformation carbon nanotube using differential quadrature method", *Struct. Eng. Mech., Int. J.*, **54**(6), 1061-1073.
Pradhan, S.C. (2012), "Nonlocal finite element analysis and small scale effects of CNTs with Timoshenko beam theory", *Finite Elem. Anal. Des.*, **50**, 8-20.
Reddy, J.N. (2007), "Nonlocal theories for bending, buckling and vibration of beams", *Int. J. Eng. Sci.*, **45**(2-8), 288-307.
Reddy, J.N. (2010), "Nonlocal nonlinear formulations for bending of classical and shear deformation theories of beams and plates", *Int. J. Eng. Sci.*, **48**(11), 1507-1518.
Reddy, J.N. and Pang, S.D. (2008), "Nonlocal continuum theories of beams for the analysis of carbon nanotubes", *J. Appl. Phys.*, **103**(2), 023511.
Reissner, E. (1984), "On a certain mixed variational theory and a proposed application", *Int. J. Numer. Methods Eng.*, **20**(7), 1366-1368.
Reissner, E. (1986), "On a mixed variational theorem and on a shear deformable plate theory", *Int. J. Numer. Methods Eng.*, **23**(2), 193-198.
Ru, C.Q. (2000), "Effect of van der Waals forces on axial buckling of a double-walled carbon nanotube", *J. Appl. Phys.*, **87**(10), 7227-7231.
Shakouri, A., Lin, R.M. and Ng, T.Y. (2009), "Free flexural vibration studies of double-walled carbon nanotubes with different boundary conditions and modeled as nonlocal Euler beams via the Galerkin

method", *J. Appl. Phys.*, **106**(9), 094307.
Sladek, J., Sladek, V., Krahulec, S., Chen, C.S. and Young, D.I. (2015), "Analyses of Circular Magnetoelectroelastic plates with functionally graded material properties", *Mech. Adv. Mater. Struct.*, **22**(6), 479-489.
Thai, H.T. (2012), "A nonlocal beam theory for bending, buckling, and vibration of nanobeams", *Int. J. Eng. Sci.*, **52**, 56-64.
Thai, H.T. and Vo, T.P. (2012), "A nonlocal sinusoidal shear deformation beam theory with application to bending, buckling, and vibration of nanobeams", *Int. J. Eng. Sci.*, **54**, 58-66.
Thostenson, E.T., Ren, Z. and Chou, T.W. (2001), "Advances in the science and technology of carbon nanotubes and their composites: a review", *Compos. Sci. Technol.*, **61**, 1899-1912.
Vinayan, B.P., Nagar, R., Raman, V., Rajalakshmi, N., Dhathathreyan, K.S. and Ramaprabhu, S. (2012), "Synthesis of graphene-multiwalled carbon nanotubes hybrid nanostructure by strengthened electrostatic interaction and its lithium ion battery application", *J. Mater. Chem.*, **22**, 9949-9956.
Wang, C.M., Tan, V.B.C. and Zhang, Y.Y. (2006a), "Timoshenko beam model for vibration analysis of multi-walled carbon nanotubes", *J. Sound Vib.*, **294**(4-5), 1060-1072.
Wang, C.M., Zhang, Y.Y., Ramesh, S.S. and Kitipornchai, S. (2006b), "Buckling analysis of micro- and nano-rods/tubes based on nonlocal Timoshenko beam theory", *J. Phys. D: Appl. Phys.*, **39**(17), 3904-3909.
Wu, C.P. and Lai, W.W. (2015a), "Reissner's mixed variational theorem-based nonlocal Timoshenko beam theory for a single-walled carbon nanotube embedded in an elastic medium and with various boundary conditions", *Compos. Struct.*, **122**, 390-404.
Wu, C.P. and Lai, W.W. (2015b), "Free vibration of an embedded single-walled carbon nanotube with various boundary conditions using the RMVT-based nonlocal Timoshenko beam theory and DQ method", *Physica E*, **68**, 8-21.
Wu, C.P. and Lee, C.Y. (2001), "Differential quadrature solution for the free vibration analysis of laminated conical shells with variable stiffness", *Int. J. Mech. Sci.*, **43**, 1853-1870.
Wu, C.P. and Tsai, Y.H. (2007), "Static behavior of functionally graded magneto-electro-elastic shells under electric displacement and magnetic flux", *Int. J. Eng. Sci.*, **45**(9), 744-769.
Wu, C.P., Hong, Z.L. and Wang, Y.M. (2017), "Geometrically nonlinear static analysis of an embedded multiwalled carbon nanotube and van der Waals interaction", *J. Nanomech. Micromech.-ASCE*, **7**, 04017012 (12 pages).
Yalcin, H.S., Arikoglu, A. and Ozkol, I. (2009), "Free vibration analysis of circular plates by differential transformation method", *Appl. Math. Comput.*, **212**, 377-386.
Yang, J., Ke, L.L. and Kitipornchai, S. (2010), "Nonlinear free vibration of single-walled carbon nanotubes using nonlocal Timoshenko beam theory", *Physica E*, **42**(5), 1727-1735.

CC